CHARACTERIZATION OF THE USNO CESIUM FOUNTAIN

Thomas B. Swanson, Eric A. Burt, and Christopher R. Ekstrom
U. S. Naval Observatory, 3450 Massachusetts Ave. NW
Washington, D.C. 20392, USA

We have performed an initial characterization of the stability of the U.S. Naval Observatory (USNO) cesium fountain atomic clock. This device has a short-term fractional frequency stability of up to $1.5\times10^{-13}\tau^{-1/2}$. This short-term performance enables us to measure hydrogen maser behavior over the short to medium term. We have recently implemented real time-steering of a hydrogen maser with the fountain. Over a period of roughly 9 days of continuous operation, we have steered out the drift of a cavity-tuned maser.

1. Introduction

Working atomic fountain clocks have now become common in the high-performance frequency standard community [1]. This is due to both the excellent stability and accuracy that these devices can achieve. At the USNO we have undertaken a program to integrate atomic fountain clocks into the USNO timing ensemble. The mission of the Observatory does not require that any of our standards be accurate realizations of the second, only that they be stable and run continuously.

The first USNO fountain based on cesium and described in this paper has essentially two goals. The first is a short-term stability of $1{-}2\times10^{-13}\tau^{-1/2}$ with a systematic floor of $1{-}3\times10^{-16}$. A consequence of this stability is that it will allow us to characterize hydrogen masers in the medium- to long-term far more precisely and rapidly than previously possible. Second, this fountain is a research device that will enable us to learn how best to optimize this technology for the specific goals of the Observatory, in particular, long-term continuous operation.

In this paper we will describe an initial characterization of the stability of this first USNO fountain, and present our first results in steering a maser with the fountain.

2. Experimental Layout

The physical layout of our fountain has been described previously [2], so we will only give a brief overview here.

We collect atoms in either a magneto-optic tarp (MOT) or optical molasses and launch them in a (1,1,1) geometry. The laser light for the upward- and downward-directed laser beams are generated by two injection-seeded tapered amplifiers. The light is then transported to the vacuum chamber with optical fibers.

The light exiting these fibers (and the detection light optical fiber) have power servos around the fiber path to reduce amplitude noise.

Our diode lasers are locked to a saturation cell in the conventional way using a fast analog integrator to control the diode piezo-electric transducer (PZT) voltage. We found that this method was insufficient to lock our lasers for more than a few days. To address this deficiency we added a digital loop that periodically polls the analog integrator and adjusts the bias PZT voltage to bring the control voltage back towards zero. This essentially gives the composite loop infinite gain at DC and keeps our lasers in lock for months at a time (with the requirement that the laser must remain single mode).

The atoms are launched in two phases, the first optimized for violent acceleration and the second for final cooling. Immediately after launch, the atoms are pumped into the F=4 hyperfine levels with a repumping laser tuned to the $F=3\rightarrow F'=4$ transition. The atoms are state-selected at the detection zone by exposure to 9.2 GHz microwaves tuned to the $|F=4,m_F=0\rangle\rightarrow|F'=3,m_F'=0\rangle$ transition. The microwaves are introduced through an axial loop antenna inside the vacuum chamber and a subsequent transit of a light sheet removes the remaining F=4 atoms.

The microwave cavity and the drift region are enclosed in a high-performance magnetic shield set providing an axial shielding effectiveness of better than 35,000 [3]. An axial solenoid provides a 225 nT magnetic field for the cavity and free precession regions.

The entire outer shield and the part of the vacuum chamber that it encloses are held at 44.5±0.1°C. As a result, everything inside the shields, including the microwave cavity, the drift region and the C-field solenoid is temperature-stabilized and gradients are minimized. Making the entire outer shield an isotherm instead of temperature-stabilizing individual components contained therein greatly reduces the sensitivity of this fountain to ambient temperature fluctuations and enhances its robustness for continuous operation. The small magnetic fields generated by the resistive heaters are kept far away from the sensitive drift region. Tests indicate no detectable perturbation to the atoms due to these fields.

After making two transits of the microwave cavity, the atoms return to the detection region. Both F=3 and F=4 atoms are detected, allowing us to calculate a transition probability, and reject atom number fluctuations. We typically run the fountain with a cycle time of 1.35 seconds.

We originally used square-wave modulation of the interrogation frequency, alternating between ±0.5 Hz from our approximately 1 Hz FWHM resonance. We found that modulating the phase of this synthesizer, leaving its frequency constant, improves the fountain's stability. The phase is changed by ±90° between the two microwave pulses that are part of each interrogation cycle. This approach is insensitive to fluctuations in launch height and is very similar to a scheme being considered for space-borne cold atom clocks to reduce their sensitivity to vibrations [4].

Our frequency chain is shown in Figure 1. The 9.2 GHz of the Dielectric Resonant Oscillator (DRO) is phase-locked to the 92nd harmonic of the 100 MHz reference input. This output is mixed with the output of a commercial direct digital synthesizer (DDS) to produce the required interrogation frequency. The various sidebands are not suppressed, but the 300 kHz linewidth of our high-Q cavity rejects these with high efficiency. This chain is simple, robust and built entirely from commercially available components. In addition, this topology allows us to insert the digital synthesizer at the top of the chain (instead of at approximately 500 MHz, as had been done previously), removing a multiplicative factor of its contributed noise. While we have not fully characterized this chain yet, it has improved the short-term stability of our fountain and reduced the upper bound on our Dick-effect [5] noise.

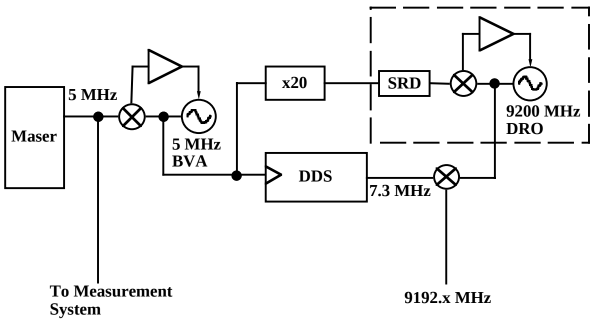

Figure 1. The new microwave frequency chain. The dashed section is a DRO-based unit that provides the phase-coherent multiplication from 100 MHz to 9.2 GHz.

Our fountain is referenced to a local cavity-tuned hydrogen maser (named N17). The steering is calculated through a single-state (frequency) Kalman filter. The frequency difference between the maser and the fountain is averaged into 5-minute data points that drive the filter. The filter has an innovation test at 4 times the current state estimate uncertainty (a form of outlier rejection). The filter also calculates critically damped steering values that would drive the frequency difference between the fountain and maser to zero.

These steering values are applied to a synthesizer, which is driven off of another 5 MHz output from the maser. This steered signal should reflect the stability of the fountain in the medium to long term. Both this steered output and the unsteered maser are measured on a local measurement system. Data from this measurement system can be easily referenced to any of the physical clocks or any of the timescales at the Observatory.

3. Results

Figure 2 shows the Allan deviation of frequency differences between the fountain and hydrogen maser N17, over a 9-day period. There are several features to note in this graph. First, the short-term stability is $1.7 \times 10^{-13}\tau^{-1/2}$. Optimizations in the operation of our frequency chain have brought this number down to $1.5\times10^{-13}\tau^{-1/2}$.

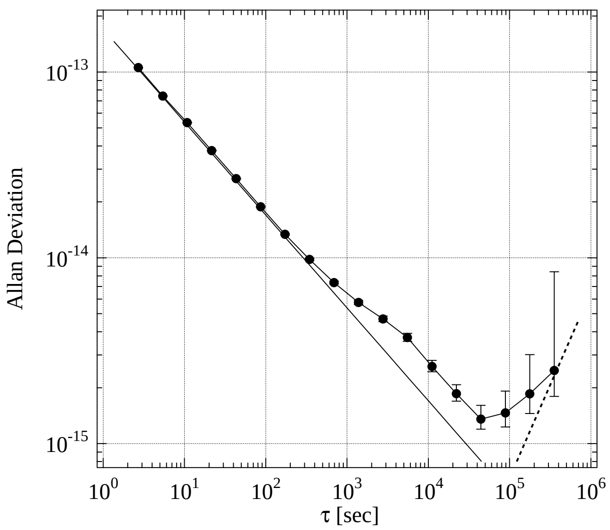

Figure 2. Allan deviation of frequency differences between the fountain and hydrogen maser N17 (filled circles). The stabilities are estimated from a continuous 9-day data set. Also shown are lines representing $1.7\text{x}10^{-13}\ \tau^{-1/2}$ (solid line), and a drift rate of $8\text{x}10^{-16}$/day (dashed line).

Second, there is a non-statistical behavior at 1000 seconds, which we suspect is due to the maser. This maser is cavity-tuned and it is well known that cavity-tuned masers can exhibit a deviation from white noise at averaging times of roughly 10^3 to 10^4 seconds. To test this we turned the cavity tuner off for N17. We expected that this would dramatically increase the drift rate, but that the deviation from white noise at 1000 seconds would disappear. The results are shown in Figure 3. The noise is completely white until it becomes dominated by the drift of about 2×10^{-14}/day. When this drift is removed, the fountain minus N17 Allan deviation is consistent with white noise.

A third feature in Figure 2 is the decrease in stability at long averaging times. This feature seems well explained by a drift rate of roughly $8\text{x}10^{-16}$/day. This drift rate was independently estimated as the drift rate of the maser N17 by comparison to internal USNO timescales, which exhibits no drift at the level of 10^{-16}/day with respect to international and local timescales.

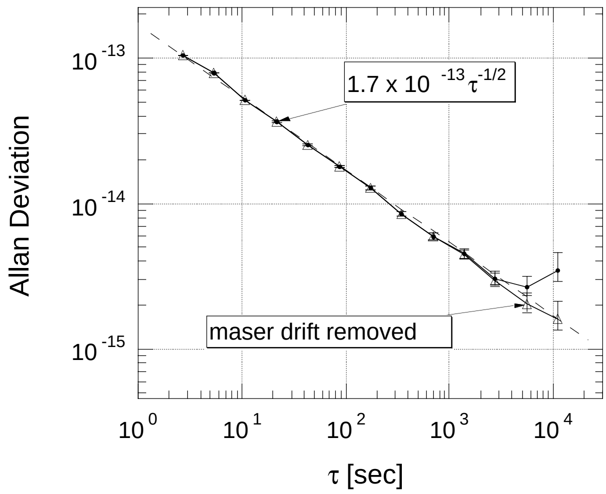

Figure 3. Allan deviation for frequency differences between the fountain and N17 with N17's cavity tuner off. The non-statistical deviation is gone at the expense of a much larger drift as expected. The closed circles show the raw data and the open triangles show those data with the drift removed.

Possible sources for the behavior near 10^5 seconds were investigated. The underlying detection process was measured by adjusting the microwave power to give two $\pi/4$ pulses with the microwaves on resonance and zero phase change. This yields a signal that is maximally insensitive to frequency fluctuations [6] and Dick-effect noise [5], and is thus a good measure of detection noise. A short-term stability of $6\times10^{-14}\tau^{-1/2}$ was measured, with no indicated floor into the mid 10^{-16}'s.

The response of the system to magnetic field fluctuations was measured using the field sensitive transition involving $|m_F|=1$ atoms. A diurnal peak, consistent with the expected magnetic field fluctuations of the Earth, was observed and makes a contribution on the clock transition of less than 1×10^{-17}.

For the entire time represented in the data set from Figure 2, the steered output of the fountain and the unsteered maser were measured in a local time interval measurement system. Figure 4 shows the results of performing a three-cornered hat analysis between the steered output of the fountain and two cavity-tuned hydrogen masers. The solutions from the masers are not shown, but are of similar stability over all averaging times in the Figure. The measurement system used for this comparison contributes white phase noise that has been measured to be $8\times10^{-13}/\tau$ and dominates the short-term noise of these solutions. Starting at an averaging time of 1000 seconds, the stability is well described by the short-term white noise properties of the fountain as measured by the unsteered maser. At long averaging times, the data exhibits a floor of 10^{-15}. This floor should be regarded as an upper bound on the performance, as over these time scales the fountain exhibited large (up to 30%) population fluctuations due to mode structure problems in one of our lasers.

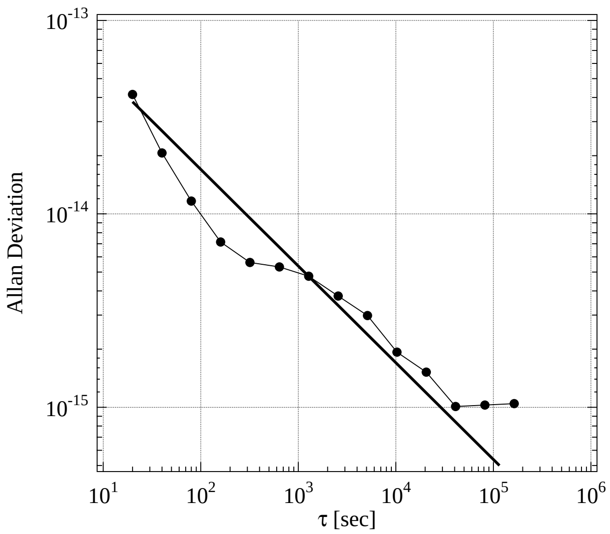

Figure 4. A three-cornered-hat solution for the steered output from the fountain (filled circles). Out to 200 seconds the data are dominated by measurement system noise ($8x10^{-13}/\tau$). The heavy line represents the white noise level of the fountain at short integration times ($1.7 \times 10^{-13}\tau^{-1/2}$, see Figure 2).

To investigate the possibility of a frequency drift in the steered fountain output, we referenced both the steered and unsteered outputs from N17 to our internal maser mean. The phase data for these comparisons are shown in Figure 5. It is clear from the hourly phase data that N17 has a significant drift rate (roughly $8x10^{-16}$/day). This is the drift rate that was indicated in Figure 2. The steered data shows no apparent drift. The phase data for both data sets has had a least-squares fit to a line removed (which will not impact estimation of a drift).

Figure 6 shows the same data as Figure 5 expressed as hourly frequencies. Both the steered (filled circles) and unsteered (open circles) data sets have had an arbitrary frequency removed. In addition, the unsteered data have been offset for clarity. There is a linear fit to each data set present in the Figure as well. The data sets and the fits clearly show that the maser N17 is drifting. The estimated residual drift of the steered output is 1.6 (1.2)$x10^{-16}$/day. If we assume we are dominated by 10^{-15} flicker noise, the error on the drift estimation would be $3.3x10^{-16}$/day [7].

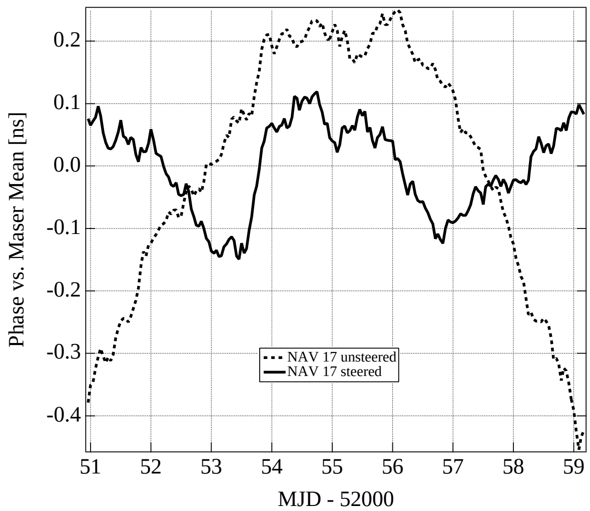

Figure 5. Phase data of both the steered output of the fountain (solid line) and unsteered N17 (dashed line) with respect to the USNO maser mean. Both data sets have a least-squares fit to a line removed. The parabolic shape of the unsteered data is characteristic of a frequency drift.

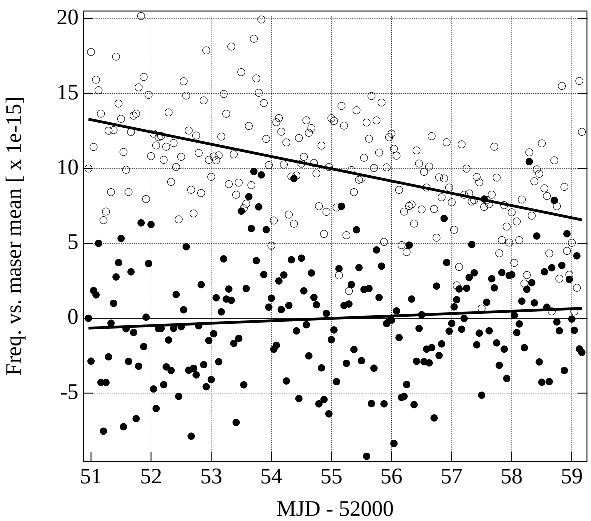

Figure 6. Hourly frequencies of the data shown in Figure 5. Both the steered (filled circles) and unsteered (open circles) data sets have had an arbitrary frequency removed and the unsteered data have been offset for clarity. The solid lines are fits to a line of each data set.

4. Conclusions

In conclusion, we have performed an initial stability analysis of the USNO cesium fountain and implemented a steered output. We have demonstrated a short-term stability of 1.5-$1.7\times10^{-13}\tau^{-1/2}$ and have shown data demonstrating that deviations from statistical behavior at around 1000 seconds are due to the maser local oscillator's cavity tuner. In the longer term we are able to establish an upper bound for the fountain "flicker floor" of 1×10^{-15}, which is probably dominated by addressable laser issues. We have also demonstrated continuous operation of the fountain, with a steered output, for 9 days and see no limitations to running the maser/fountain combination in steered mode for 1 month or more. Thus, we have reached the short- and medium-term stability goals for this device, as well as the goal of being able to measure short- to medium-term maser performance and continue to analyze long-term behavior. In addition, we have laid the basis for future continuously operating USNO fountains.

References

1. Clairon A., *et al.*, in *Proceedings of the Fifth Symposium on Frequency Standards and Metrology* (1995), 49-59; Bize S., *et al.,* 9-11; Jefferts S. R., *et al.*, 12-15; Weyers S., *et al.*, 16-19, P. B. Whibberly, 24-26, all in *Proceedings of the conference EFTF and IEEE FCS* (1999); Swanson T., *et al.*, in *Proceedings of the 2000 IEEE/EIA International Frequency Control Symposium* (2000), 672-675; Levi F., *et al.*, 104-107 and Joyet, A. *et al.*, 72-76, both in *Proceedings of the 15th European Frequency and Time Forum* (2001).
2. Ekstrom C., *et al.*, in *Proceedings of the 14th European Frequency and Time Forum* (2000), 502-504.
3. Swanson T., *et al.*, in *Proceedings of the 2000 IEEE/EIA International Frequency Control Symposium* (2000), 672-675.
4. Klipstein W.M., *et al.*, in *Proceedings of the 2001 IEEE International Frequency Control Symposium* (2001), 25-32.
5. Dick G. J., in *Proceedings of the 19th PTTI Applications and Planning Meeting* (1987), 133-147.
6. Santarelli G., *et al.*, *Phys. Rev. Lett.* **82** (1999), 4619-4622.
7. Greenhall C.A., in *Proceedings of the 1997 IEEE International Frequency Control Symposium* (1997), 428-432.